Lens Distortion Model Estimation by Minimizing Line Reprojection Errors

Daniel Santana-Cedrés, Luis Gomez *Member, IEEE*, Miguel Alemán-Flores, Agustín Salgado, Julio Esclarín, Luis Mazorra, and Luis Alvarez

Abstract—Most techniques for camera calibration using planar calibration patterns require the computation of a lens distortion model and a homography, given by a 3×3 matrix. Both are simultaneously refined using a bundle adjustment, which minimizes the reprojection error of a collection of points (usually the corners of the rectangles of a calibration pattern) when projected from the image onto the camera sensor. If the lens shows a significant distortion, the location and matching of the corners can be difficult and inaccurate. To cope with this problem, instead of point correspondences, we propose to use line correspondences to compute the reprojection error. We have designed a fully automatic algorithm to estimate the lens distortion model and the homography by computing line correspondences and minimizing the line reprojection error. In the experimental setup we focus on the analysis of the quality of the obtained lens distortion model. We present some experiments which show that the proposed method outperforms the results obtained by the standard methods to compute lens distortion models based on line rectification.

Index Terms—camera sensor, lens distortion, homography estimation, reprojection error

1 Introduction

Lens distortion is an optical aberration which causes straight lines in the scene to be projected onto the image as distorted lines. To measure the amount of lens distortion, professional commercial software, such as Imatest (http://www.imatest.com/) or DxO (http://www.dxomark.com), proposes to measure how far the distorted lines in the image are from being straight lines. The lens distortion profile is usually modeled using a radial model given by the general equation:

$$\begin{pmatrix} \hat{x} - x_c \\ \hat{y} - y_c \end{pmatrix} = L(r) \begin{pmatrix} x - x_c \\ y - y_c \end{pmatrix}, \quad (1)$$

where (x_c, y_c) represents the distortion center, (x, y) is a point in the image domain, $(\hat{x}, \hat{y})$ is the transformed (distortion-free) point, $r = \|(x, y) - (x_c, y_c)\|$, and $L(r)$ represents the shape of the distortion model. Two types of radial lens distortion models are the most frequently applied in computer vision due to their excellent trade-off between accuracy and easy calculation: the polynomial model and the division model. The polynomial model is formulated as

$$L(r) = 1 + k_1 r^2 + k_2 r^4 + .. + k_n r^{2n}, \quad (2)$$

whereas the division model is formulated as

$$L(r) = \frac{1}{1 + k_1 r^2 + k_2 r^4 + .. + k_n r^{2n}}. \quad (3)$$

- *D. Santana-Cedrés, M. Alemán-Flores, A. Salgado, J. Esclarín, L. Mazorra, and L. Alvarez are with the CTIM, Departamento de Informática y Sistemas, Universidad de Las Palmas de Gran Canaria, 35017, Las Palmas, Spain.*
  E-mail: {dsantana, maleman, asalgado, jesclarin, lmazorra, lalvarez }@ctim.es
- *L. Gomez is with the CTIM, Departamento de Ingeniería Electrónica y Automática, Universidad de Las Palmas de Gran Canaria, 35017, Las Palmas, Spain.*
  E-mail:lgomez@ctim.es

*Manuscript received ****, ***; revised ***, ****

The distortion center (x_c, y_c) and the distortion parameters $\{k_1, .., k_n\}$ are usually estimated in order to minimize a line rectification error. Once the lens distortion model is fully estimated, it can be applied to the image to correct the lens distortion. Commercial software, like Imatest or DxO, proposes to use a flat calibration pattern to estimate lens distortion models. For each lens available in the market, images of the calibration pattern are taken for most of the lens/camera configurations (including the different focal lengths in the case of zoom lens). From these images, the lens distortion models are computed and all this information is stored in a large database. When a user wants to correct the lens distortion of an image, the algorithm uses the image EXIF metadata to get the lens/camera configuration and to choose, in the stored database, the lens distortion model to be applied for the correction. This approach has the advantage that the distortion models are computed using calibration patterns, for which accurate estimations can be obtained and the resulting models can be applied to any image acquired with the same lens configuration. In particular, distortion correction can also be applied to images with no visible lines. However, using a line rectification criterion to estimate the distortion model does not exploit the metric information provided by calibration patterns, where we know the exact position of each line in the pattern. To exploit such metric information we need to take into account the plane homography H given by a 3×3 matrix. The combination of the homography and the lens distortion model fully determines the way the calibration pattern is projected onto the camera sensor. We point out that the lens distortion model is an internal camera feature that is usually assumed to be independent of the particular location or orientation of the camera. That is, if we take several images of the calibration pattern from different locations and orientations, we can assume that all cameras share the same lens distortion model, but with different homographies. In fact, this is a simplification because, as shown in [1], the lens distortion model depends slightly on the distance at which the camera is focused, so that it is not completely independent of the camera location in the scene.

In this paper, we propose a new method to compute the lens distortion model and the homography based on the minimization of the line reprojection error. We use a nonlinear minimization technique which requires a parameter initialization, in such a way that we also have to deal with the problem of lens distortion model and homography initialization. On the other hand, in order to properly define the line reprojection error, we need to match the lines of the calibration pattern with the distorted lines projected onto the camera sensor.

Once the lens distortion model and the homography have been estimated, we can perform further 3D calibration procedures. For instance, if several images of the calibration pattern taken with the same camera are available, we can use the well-known Zhang technique introduced in [2] to compute all internal and external parameters of the cameras. However, in the experimental setup of this paper we do not focus on 3D calibration procedures, we focus on the analysis of the quality of the lens distortion model obtained with the proposed method which is an internal feature of the camera.

The rest of the paper is organized as follows : In section 2, we present some related works. In section 3, the proposed method is explained. Section 4 shows some experiments using a calibration pattern. Finally, in section 5, we present some conclusions.

2 Related Works

Commercial lenses can show several optic aberrations like field curvature (see for instance [3]) or lens distortion. Radial distortion models are commonly used in the literature to model the lens distortion aberration. In the seminal paper [4], the author introduces the general shape of polynomial lens distortion models. Division models were initially proposed in [5], but have received special attention after the research by Fitzgibbon [6]. The main advantage of the division model is the requirement of fewer terms than the polynomial model to cope with images showing severe distortion. Therefore, the division model seems to be more suitable for wide-angle lenses (see a recent review on distortion models for wide-angle lenses in [7]). In [8] and [9], a detailed analysis of high order models is presented, including polynomial and division models. Moreover, in the case of real images, the authors evaluate the accuracy of the lens distortion model by extracting and matching points using the SIFT method in an image of a highly textured pattern. A homography to match the camera projection as well as the lens distortion parameter are then estimated by minimizing the reprojection error. The minimization of the reprojection error is also a standard tool in camera calibration. In the seminal paper [2], the reprojection error is used to optimize camera calibration parameters.

Most of the methods to estimate lens distortion models are based on distorted line rectification. This approach is used, for instance, in [10], [11], [12] and [1]. New automatic methods without user intervention have recently emerged. In [13], an automatic method to estimate radial distortion models is presented. In [14] and [15], the authors present a detailed study about calibration harp reliability in the context of high-precision camera distortion measurements. In [16], the authors present a detailed study about different models for lens distortion aberrations. In [17], the authors introduce a metric measure of lens distortion using the projective cross ratio invariance. In [18], [19], the authors propose an improvement of the calibration procedure proposed in [2] for a collection of images, by decoupling the lens distortion and the camera parameter estimations. In [20], the authors propose a method to estimate radial distortion models based on the epipolar constraint. In [21], authors propose a method for the automatic estimation of radial lens distortion using several geometric constraints like rectilinear elements and vanishing points. In [22], authors introduce a method for the calibration of wide angle lens cameras where points locations in the images are corrected using geometric constraint and the lens distortion model is computed by minimizing a point reprojection error.

In this paper, we use two-parameter radial models due to their simplicity and accuracy. In previous works (see [23] and [24]), we have introduced a method to estimate two-parameter models which is able to cope with a high distortion level. The method is based on the estimation of distorted lines in the images. The outcomes of this method are:

1) A collection of distorted lines $\{l_k\}_{k=1,\ldots,N_{lines}}$ detected in the image.
2) For each distorted line k, a collection of edge points $\{x_{k,j}\}_{j=1,\ldots,N_k}$ belonging to the distorted line.
3) A two-parameter distortion model $\mathbf{u} = (x_c, y_c, k_1, k_2)$ computed by line rectification.

These outcomes will be used in the method we propose in this paper.

3 Proposed Method

In fig. 1, we show an image of the calibration pattern we use acquired with a Tokina DX 11-16mm lens showing a high distortion. We observe that the calibration pattern consists of a collection of straight lines $\{l'_{k'}\}_{k'=1,\ldots,N'_{lines}}$ given by the edges of the squares. We also point out that we have included 3 colored squares in the center of the calibration pattern, that we will use as reference system.

In the case of a distortion-free lens, the camera follows the well-known pinhole model and, for any plane in the scene, there exists a homography H which projects the image plane onto the 3D plane. That is, if $\overline{x} = (x, y)$ is an image point, then its projection $\overline{x}'(\overline{x}, H)$ in the 3D plane is given by

$$x'(\overline{x}, H) = \frac{h_{00}x + h_{01}y + h_{02}}{h_{20}x + h_{21}y + h_{22}} \quad (4)$$

$$y'(\overline{x}, H) = \frac{h_{10}x + h_{11}y + h_{12}}{h_{20}x + h_{21}y + h_{22}}. \quad (5)$$

If the lens suffers from distortion aberration, we need to correct the lens distortion before applying the above projection equation. We denote by $\mathbf{u} = (x_c, y_c, k_1, k_2)$ the parameters of the distortion model (the distortion center and

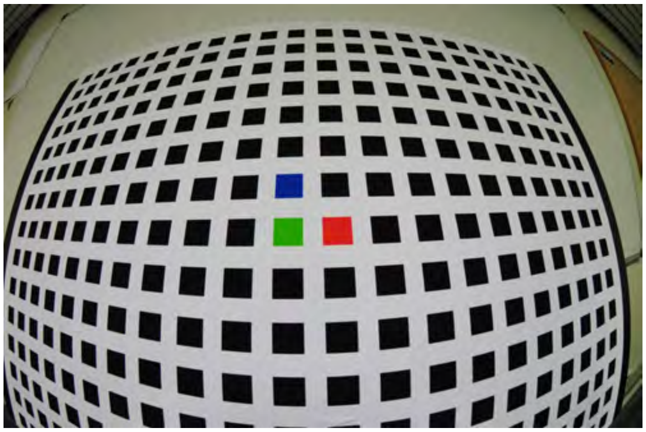

Fig. 1. Image of the calibration pattern we use taken with a Tokina DX 11-16mm lens showing a high distortion.

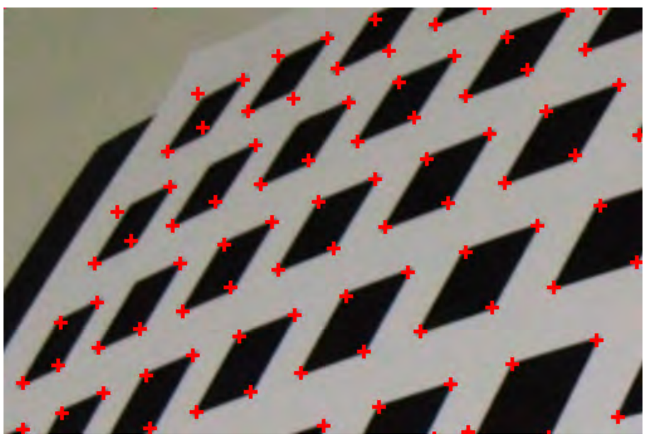

(a)

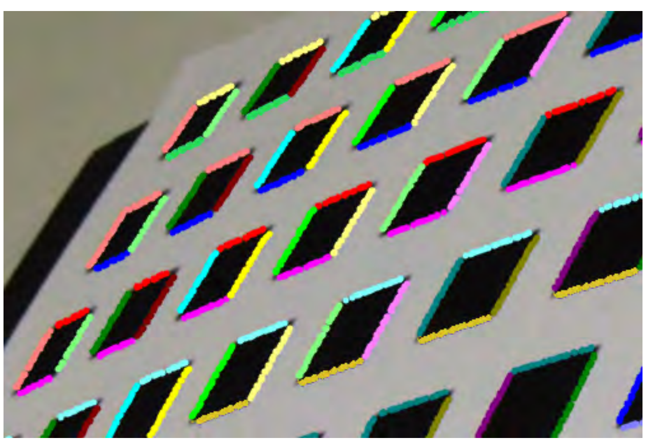

(b)

Fig. 2. We present a zoom of the calibration pattern. In (a) the corner locations estimated using Harris method are shown. In (b) some points of the lines used to compute the line reprojection error are shown.

the distortion parameters k_1, k_2). Given a point $\overline{x} = (x, y)$ in the image, we denote by $\hat{\overline{x}}^{\mathbf{u}} = (\hat{x}^{\mathbf{u}}, \hat{y}^{\mathbf{u}})$ the corrected point using the model given by $\mathbf{u}$, which is computed by the evaluation of equation (1). Then, by introducing the lens distortion correction in the previous projection equation, we obtain that

$$\bar{x}'(\bar{x}, H, \mathbf{u}) = \begin{pmatrix} \dfrac{h_{00}\hat{x}^{\mathbf{u}}+h_{01}\hat{y}^{\mathbf{u}}+h_{02}}{h_{20}\hat{x}^{\mathbf{u}}+h_{21}\hat{y}^{\mathbf{u}}+h_{22}} \\ \dfrac{h_{10}\hat{x}^{\mathbf{u}}+h_{11}\hat{y}^{\mathbf{u}}+h_{12}}{h_{20}\hat{x}^{\mathbf{u}}+h_{21}\hat{y}^{\mathbf{u}}+h_{22}} \end{pmatrix}. \qquad (6)$$

The method we propose in this paper can be divided into the following steps :

1) We apply the method proposed in [23] to obtain the distorted lines $\{l_k\}_{k=1,\ldots,N_{lines}}$, their associated points $\{x_{k,j}\}_{j=1,\ldots,N_k}$ and an initial estimation $\mathbf{u} = (x_c, y_c, k_1, k_2)$ for the lens distortion model.
2) We detect the colored squares in the image to fix a reference system.
3) Using the reference system given by the colored squares, we match the distorted lines $\{l_k\}$ in the image with the straight lines $\{l'_{k'}\}$ in the actual calibration pattern, obtaining a collection of corresponding lines $\{(l_{k_n}, l'_{k'_n})\}_{n=1,\ldots,N}$ and a first estimation of the homography H.
4) We optimize H and u by minimizing the line reprojection error given by

$$E(H, \mathbf{u}) = \sum_{n=1}^{N} \sum_{j=1}^{N_{k_n}} \Big(distance(\bar{x}'(\bar{x}_{k_n,j}, H, \mathbf{u}), l'_{k'_n}) \Big)^2 \qquad (7)$$

We point out that the usual approach to compute the reprojection error is based on point correspondences. The location of the corners of the squares of the projection of the calibration pattern in the camera sensor are estimated and then matched with the corners of the actual calibration pattern. However, in the case of a high distortion level, the estimation of the location of the corners in the image can be difficult and inaccurate. One of the main novelties of our approach is that we do not use corner estimations, and we express the reprojection error in terms of the edge points associated to the distorted lines, which is more robust. In fig. 2 we illustrate the advantage of our approach showing a zoom area of an image of the calibration pattern, in fig. 2(a) we show the corner locations obtained using the standard Harris method. We point out that the lens distortion can strongly modify the square shapes and the Harris method can provide quite inaccurate results because corner curvature can be very high or very low, and in both cases corner detection techniques provide inaccurate results. In the case of high curvatures, the location of the detected corner is displaced with respect to its actual location and in the case of low curvature the corner can not even be detected or the result can be completely wrong. We also point out that a high amount of lens distortion can make very difficult the procedure to match the corners in the image with the corner in the calibration pattern. In 2(b) we illustrate the edge point collection associated to the lines we use to perform the line reprojection. These edge points and lines has been obtained using the method introduced in [23] (in fact, in this method edge points with high curvature are removed to improve the accuracy of edge point location). We observe that the location of the edge points is much more accurate than the location of the corners. Moreover each line is defined by a large collection of edge points which provide a very robust definition of the line.

Next we will explain the different steps of the proposed method in more detail:

Step 1: Initial estimation of the distorted lines and the lens distortion model. We use the method proposed in [23], where we introduced a technique for the automatic estimation of two-parameter radial distortion models, considering polynomial as well as division models. The method first detects the edge points using the Canny edge detector. Then, from the edge points, and by applying the Hough transform enriched with a radial distortion parameter, we extract the collection $\{l_k\}_{k=1,\dots,N_{lines}}$ of the longest distorted lines within the image and their associated edge points $\{x_{k,j}\}_{j=1,\dots,N_k}$. From these lines, the first distortion parameter is estimated. Afterward, we initialize the second distortion parameter to zero and the two-parameter model is embedded into an iterative nonlinear optimization process to improve the estimation by minimizing a line rectification error. This error is defined in the following way: given a lens distortion model determined by the parameter vector $\mathbf{u}$, we define the undistorted line corresponding to each distorted line l_k by minimizing the following distance error:

$$(\alpha_k^{\mathbf{u}}, d_k^{\mathbf{u}}) = arg\ \min_{\alpha,d} \sum_{j=1}^{N_k} \left(cos(\alpha)\hat{x}_{kj}^{\mathbf{u}} + sin(\alpha)\hat{y}_{kj}^{\mathbf{u}} + d \right)^2, \quad (8)$$

where $(\alpha_k^{\mathbf{u}}, d_k^{\mathbf{u}})$ represents the orientation and the distance to $(0,0)$ for the straight line which minimizes the square distance from the corrected edge points to such line. This well-known minimization problem has a simple close-form solution (see for instance [25] for more details).

The line rectification error associated to the lens distortion model given by the vector parameter $\mathbf{u}$ is then defined as

$$E(\mathbf{u}) = \frac{\sum_{\mathbf{k=1}}^{\mathbf{Nlines}} \sum_{\mathbf{j=1}}^{\mathbf{N_k}} \left(\mathbf{cos}(\alpha_{\mathbf{k}}^{\mathbf{u}})\hat{\mathbf{x}}_{\mathbf{kj}}^{\mathbf{u}} + \mathbf{sin}(\alpha_{\mathbf{k}}^{\mathbf{u}})\hat{\mathbf{y}}_{\mathbf{kj}}^{\mathbf{u}} + \mathbf{d}_{\mathbf{k}}^{\mathbf{u}} \right)^{\mathbf{2}}}{\sum_{\mathbf{k=1}}^{\mathbf{N_{lines}}} \mathbf{N_k}}. \quad (9)$$

This optimization aims at reducing the distance from the edge points to the lines, adjusting two distortion parameters as well as the coordinates of the center of distortion. In fig. 3(a), we illustrate the initial collection of distorted lines obtained by applying this method to the image in fig. 1. An important advantage of this method is that it can deal with high distortion levels. However, the line rectification error (9) does not exploit the knowledge of the scene that we have when we deal with a calibration pattern, where we know the exact location of all lines in the scene. Furthermore, it does not take into account if, after the distortion correction, the undistorted lines are the projection onto the image of the actual lines in the calibration pattern. This is the main motivation for the introduction, in this paper, of the line reprojection error (7) in order to obtain a more accurate model estimation.

Step 2: Detection of the colored squares in the image. The calibration pattern we use includes 3 colored squares in red, green and blue in the center. To obtain the location of such colored squares in the image, we first transform the original RGB image channels in the following way:

$$\begin{cases} R_{new} = max\{\ 0\ ,\ R - max\{G, B\}\ \} \\ G_{new} = max\{\ 0\ ,\ G - max\{R, B\}\ \} \\ B_{new} = max\{\ 0\ ,\ B - max\{R, G\}\ \} \end{cases}$$

Then we convolve the resulting image with a Gaussian kernel. The locations of the maxima of these channels in the new image correspond to points inside the colored squares. In fig. 3(b), we illustrate the result of this image transformation and the location of the maxima of the channels using the image in 1(b). This technique has also been used in [26], in the context of automatic corner matching in Zhang's calibration pattern.

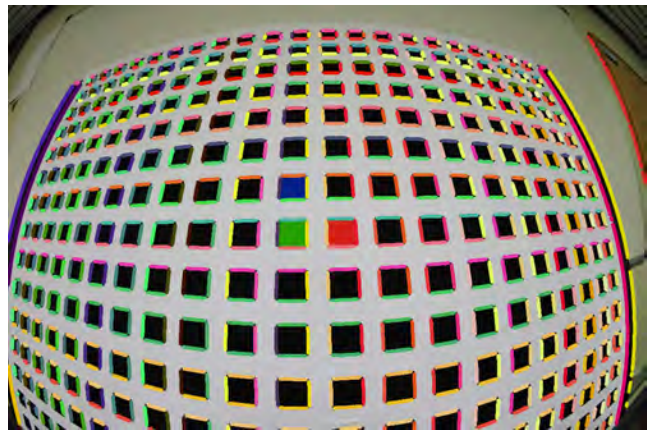

(a)

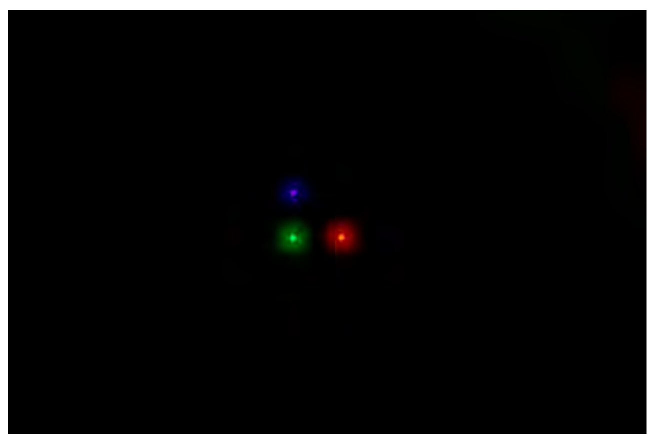

(b)

Fig. 3. (a) Illustration of the collection of distorted lines obtained using the method proposed in [23], (b) Illustration of image transformation to obtain the location of the colored squares.

Step 3: Matching of the lines in the calibration pattern with their projections onto the image. First estimation of the homography H. Once the locations of the colored squares have been computed, we can match the lines passing through the edges of such squares and their corresponding ones in the actual calibration pattern. From this line matching, we can compute a first estimation of the homography using an algebraic close-form solution of homography estimation from point or line matching (see [25], [27], or [28] for more details). Once we obtain a first estimation of H, we use it to enlarge the number of line matchings by projecting each distorted line in the actual calibration pattern. By using a proximity criterion, we identify pairs consisting of a line in the calibration pattern and its projection in the image. This is an incremental procedure because, when new line matchings are found, we can recompute the homography H using all the line matchings which have been obtained.

Step 4: Optimization of the lens distortion model and the homography H by minimizing the line reprojection error. We use the Levenberg-Marquardt algorithm to minimize the reprojection error (7) with respect to the distortion model $\mathbf{u} = (x_c, y_c, k_1, k_2)$ and the homography H using the distortion model obtained in step 1 and the homography obtained in step 3 as initial guess. The coefficients of the homography H are of very different nature and a small variation in some of such coefficients can produce large variations in the reprojection error. For this reason, instead of using the coefficients of H as parameters of the minimization algorithm, we use the locations of the projections of the corners of the green square onto the image. This provides 8 parameters (the coordinates of the 4 corners in the image) and the homography can easily be estimated from such parameters (see for instance [25] for more details).

4 Experimental results

The estimation of the lens distortion model and the homography can be used to perform further 3D calibration procedures. In particular, if we take several pictures of the calibration pattern from different locations, we can use the well-known Zhang technique introduced in [2] to compute all internal and external parameters of the cameras. However, in the experimental setup of this paper we do not focus on 3D calibration procedures, we focus on the analysis of the quality of the obtained lens distortion model using a single image. We are going to compare the results obtained by the following 5 lens distortion estimation methods:

- E_{rec}^{Ima} : two-parameter polynomial model provided by Imatest commercial software based on line rectification.
- E_{rec}^{P2p} : two-parameter polynomial model obtained by the method introduced in [23] based on line rectification.
- E_{rec}^{D2p} : two-parameter division model obtained by the method introduced in [23] based on line rectification.
- E_{rep}^{P2p} : two-parameter polynomial model obtained by minimizing the reprojection error (7).
- E_{rep}^{D2p} : two-parameter division model obtained by minimizing the reprojection error (7).

We study the accuracy of the different methods for a variety of commercial lenses. In table 1, we show, for the first 3 methods, the line rectification error given by equation (9) and, for the last 2 methods, the reprojection error (7). In the first row of the table, we present the information about the lens and the focal length fixed (in parentheses) in the case of zoom lenses. For the methods E_{rec}^{Ima}, E_{rec}^{P2p} and E_{rec}^{D2p}, the error is expressed in pixels using formula (9). For the methods E_{rep}^{P2p} and E_{rep}^{D2p}, the error is expressed in mm using formula (7). In this case, we show the final reprojection error after minimization of (7) and, in parentheses, the original reprojection error obtained using the methods E_{rec}^{P2p} and E_{rec}^{D2p} respectively. For the rectification error and the reprojection error models, we emphasize the model with the lowest error in bold. We point out that, in the case of Tokina lens, which presents a high level of distortion, Imatest software is not able to provide a lens distortion model and, for the other lenses, the rectification error obtained in [23] is much lower that the one computed using Imatest software. We also observe that the minimization of the reprojection error (7) reduces, in a significant way, the original reprojection error computed using the lens distortion model provided by the rectification method. We observe that, for the Tokina DX 11-16mm lens, which shows a high distortion level, the error provided by the division model is significantly lower than that obtained by the polynomial model. However, for the rest of the lenses, which present a moderate amount of distortion, the polynomial model is slightly better than the division one.

	Error				
Lens	E_{rec}^{Ima}	E_{rec}^{P2p}	E_{rec}^{D2p}	E_{rep}^{P2p}	E_{rep}^{D2p}
Tokina 11-16 (11)	-	3.594	**0.784**	0.503 (8.855)	**0.144** (0.187)
Sigma 8-16 (8)	20.25	**2.668**	2.915	**0.366** (0.538)	0.402 (0.522)
Sigma 8-16 (12)	7.11	**1.833**	1.853	**0.243** (0.408)	0.246 (0.344)
Nikkor 14-24 (14)	3.87	**0.430**	0.434	**0.085** (0.120)	0.086 (0.118)
Nikkor 14-24 (18)	2.82	**0.273**	0.273	**0.057** (0.074)	0.057 (0.097)
Nikkor 17-35 (17)	3.66	**1.304**	1.340	**0.241** (0.433)	0.247 (0.361)
Nikkor 24-70 (24)	2.97	**0.337**	0.338	**0.075** (0.105)	0.076 (0.102)

TABLE 1
Errors obtained by the different methods in a variety of commercial lenses.

In tables 2 and 3, we show the coefficients of the distortion model obtained for the different methods. As proposed in Imatest software, we express the distortion coefficients in "normalized in center-corner" units, given by the expressions

$$\tilde{k}_1 = r_{max}^2 k_1, \qquad \tilde{k}_2 = r_{max}^4 k_2,$$

where r_{max} is the maximum distance from the distortion center to the image domain corners. These normalized values are independent of the image resolution. In fig. 4 we show the plotting of the function $L(r)$ given by the equation (2) or (3), in normalized coordinates, obtained using different lens distortion estimation methods for the Tokina DX 11-16mm lens and the Nikkor 17-35mm lens. The Tokina lens shows a high level of distortion, the Imatest software fails to estimate a lens distortion model and we can observe in the plotting that the polynomial models are not able to cope with such high amount of distortion. In this case, the line reprojection error is much lower using division model than polynomial models. The Nikkor lens shows a moderate levels of distortion and in this case the plotting of the function $L(r)$ is similar for polynomial and division models except in the case of the model provided by Imatest software which is quite different and shows a high rectification error.

To illustrate the profile of the obtained lens distortion models for each lens, we use the representation showed in fig. 5, where the profile of the Tokina DX 11-16mm lens is presented using a 11 focal length and the division model. In this profile, the bright lines represent a lattice of the 3D

	$\tilde{k}_1$				
Lens	E_{rec}^{Ima}	E_{rec}^{P2p}	E_{rec}^{D2p}	E_{rep}^{P2p}	E_{rep}^{D2p}
Tokina 11-16 (11)	-	0.472	-0.594	0.397	-0.587
Sigma 8-16 (8)	0.001	-0.011	-1.8×10^{-5}	-0.001	-0.005
Sigma 8-16 (12)	-0.026	-0.037	0.034	-0.032	0.031
Nikkor 14-24 (14)	0.069	0.077	-0.075	0.078	-0.079
Nikkor 14-24 (18)	0.019	0.034	-0.033	0.033	-0.033
Nikkor 17-35 (17)	0.105	0.128	-0.127	0.132	-0.126
Nikkor 24-70 (24)	0.043	0.060	-0.061	0.058	-0.059

TABLE 2
Value for parameter $\tilde{k}_1$ of the lens distortion models in a variety of commercial lens. The value is normalized in center-corner units.

	$\tilde{k}_2$				
Lens	E_{rec}^{Ima}	E_{rec}^{P2p}	E_{rec}^{D2p}	E_{rep}^{P2p}	E_{rep}^{D2p}
Tokina 11-16 (11)	-	0.992	-0.158	1.129	-0.172
Sigma 8-16 (8)	0.051	0.106	-0.090	0.096	-0.084
Sigma 8-16 (12)	0.032	0.065	-0.062	0.059	-0.058
Nikkor 14-24 (14)	0.002	0.012	-0.008	0.012	-0.004
Nikkor 14-24 (18)	0.007	0.002	0.001	0.003	-0.002
Nikkor 17-35 (17)	-0.041	-0.053	0.057	-0.057	0.057
Nikkor 24-70 (24)	0.006	0.004	-0.0002	0.007	-0.003

TABLE 3
Value for parameter $\tilde{k}_2$ of the lens distortion models in a variety of commercial lenses. The value is normalized in center-corner units.

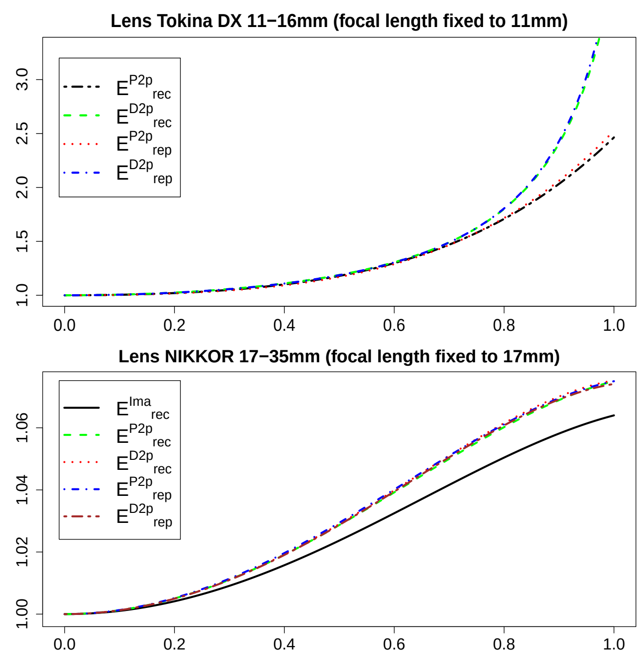

Fig. 4. Plot of the function $L(r)$ in normalized coordinates, obtained using different methods, for 2 commercial lens.

scene covered by the camera, and the dark lines represent the projection of such lines onto the image.

In fig. 6, 7 and 8, we illustrate the lens distortion profile for a variety of lenses. For each lens configuration, we show a picture acquired with the lens as well as the lens distortion profile obtained using this picture.

Assuming, as usual, that the lens distortion model is a camera internal parameter independent of the camera location in the space we can apply the estimated distortion model using the calibration pattern to correct the distortion of any image taken with the same camera configuration.

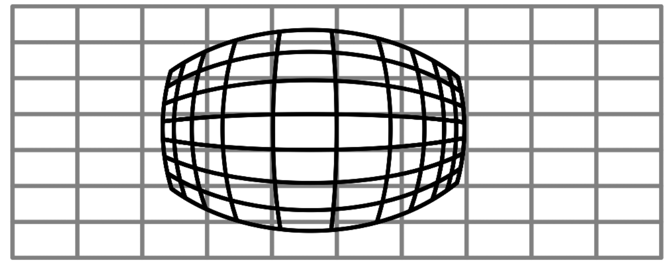

Fig. 5. Illustration of Tokina DX 11-16mm lens distortion profile (with the focal length fixed to 11) estimated using the method proposed in this paper and division models. The bright lines represent a lattice of the 3D scene covered by the camera and the dark lines represent the projection of such lines onto the image.

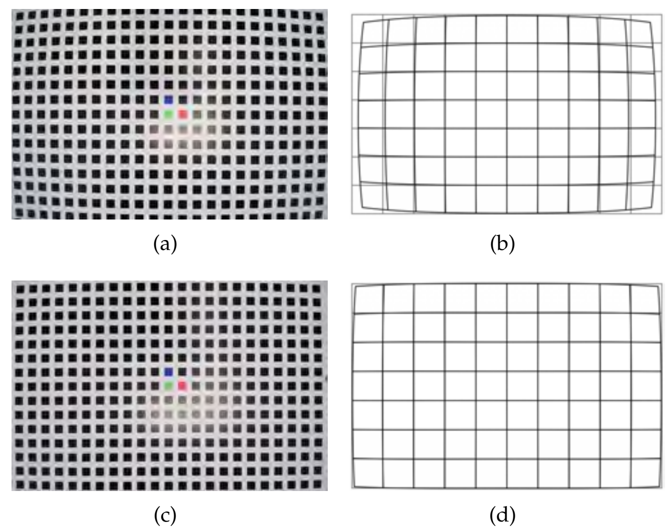

Fig. 6. Lens distortion model estimation of the lens Sigma DX 8-16 mm mounted in a Nikon D90 camera. We present the picture taken with the camera and the obtained lens distortion model profile. In (a)–(b) we fixed the focal length to 8 and in (c)–(d) we fixed the focal length to 12.

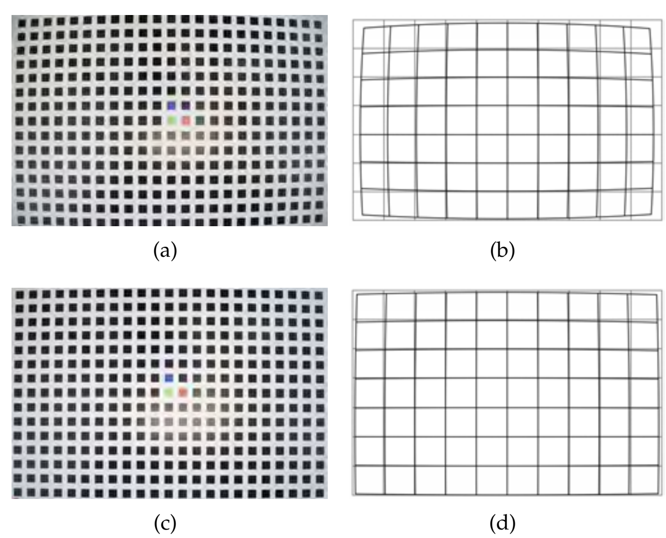

Fig. 7. Lens distortion model estimation of the lens Nikkor 14-24 mm mounted in a Nikon D800 camera. We present the picture taken with the camera and the obtained lens distortion model profile. In (a)–(b) we fixed the focal length to 14 and in (c)–(d) we fixed the focal length to 18.

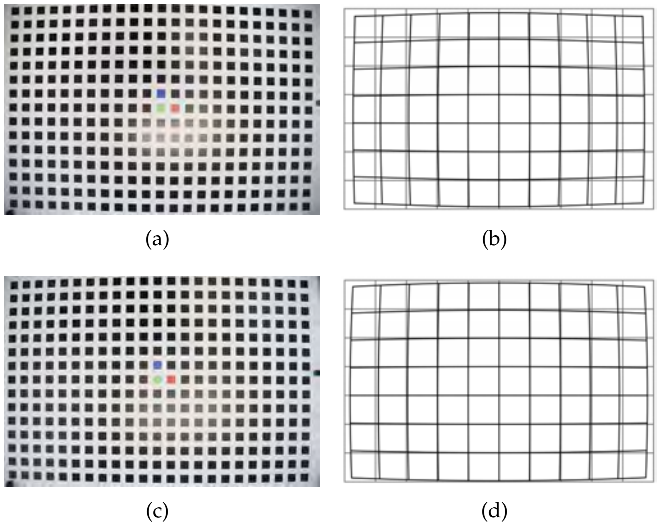

Fig. 8. In (a)–(b) we show the picture and the profile of the lens Nikkor 17-35mm mounted in a Nikon D800 camera with a focal length equal to 17. In (c)–(d) we show the picture and the profile of the lens Nikkor 24-70mm mounted in a Nikon D800 camera with a focal length equal to 24.

This is illustrated in fig. 9 where present the results of the lens distortion correction of some photos taken with the Tokina DX 11-16mm lens (with the focal length fixed to 16mm) using the lens distortion model computed using the picture of the calibration pattern which is also included in fig. 9. We point out that the real images showed in fig. 9 contain very few and short visible lines so the lens distortion estimation methods based on line detection and rectification are not expected to work properly.

Fig. 9. Lens distortion correction using the lens distortion model obtained from the calibration pattern using the proposed method. On the left we show the original image and on the right the corrected one.

5 Conclusions

The main contribution of this paper is a new technique based on the minimization of a line reprojection error to compute simultaneously the lens distortion model and the homography which project a calibration pattern in the camera sensor. The main advantage of this method is that the information we can extract from the image about the lines is more robust and accurate than the one we obtain using corner detectors specially in the case the lens shows a high level of distortion. We design a fully automatic algorithm to estimate the lens distortion model and the homography and we present some experiments which shows that the estimated lens distortion model outperforms the results obtained with the usual methods based on line rectification. The main limitation of the usual line rectification techniques is that they are not based on a metric measure and they do not exploit the knowledge we have about the line location in the calibration pattern. The method we propose is more accurate because it is based on the minimization of a metric distance measuring the match between the lines in the calibration pattern and their projection in the camera sensor. So the proposed method represents a more accurate alternative to the usual way lens distortion is evaluated in commercial lenses. We also show how the lens distortion model estimated using the calibration pattern can also be applied to correct the distortion of any image taken with the same lens.

References

[1] L. Alvarez, L. Gomez, and R. Sendra, “Accurate depth dependent lens distortion models: An application to planar view scenarios,” *Journal of Mathematical Imaging and Vision*, vol. 39, no. 1, pp. 75–85, 2011.

[2] Z. Zhang, “A flexible new technique for camera calibration,” *IEEE Transactions on Pattern Analysis and Machine Intelligence*, vol. 22, no. 11, pp. 1330–1334, 2000.

[3] Y. Zhang, I. Minema, L. G. Zimin, and T. Ueda, “Analysis of radially restored images for spherical single lens cellphone camera,” *IEEE Sensors Journal*, vol. 11, no. 11, pp. 2834–2844, Nov 2011.

[4] D. Brown, “Close-range camera calibration,” *Photogrammetric Engineering*, vol. 37, no. 8, pp. 855–866, 1971.

[5] R. Lenz, “Linsenfehlerkorrigierte Eichung von Halbleiterkameras mit Standardobjektiven für hochgenaue 3D - Messungen in Echtzeit,” in *Mustererkennung 1987*, ser. Informatik-Fachberichte, E. Paulus, Ed. Springer Berlin Heidelberg, 1987, vol. 149, pp. 212–216.

[6] A. W. Fitzgibbon, “Simultaneous linear estimation of multiple view geometry and lens distortion,” *In: Proc. IEEE International Conference on Computer Vision and Pattern Recognition*, pp. 125–132, 2001.

[7] C. Hughes, M. Glavin, E. Jones, and P. Denny, “Review of geometric distortion compensation in fish-eye cameras,” in *Signals and Systems Conference, 208. (ISSC 2008). IET Irish*, Galway, Ireland, 2008, pp. 162–167.

[8] T. Zhongwei, R. Grompone, P. Monasse, and J. M. Morel, “Self-consistency and universality of camera distortion models,” *In hal-00739516, version 1*, pp. 1–8, 2012.

[9] R. Grompone, P. Monasse, J. M. Morel, and Z. Tang, "Towards high-precision lens distortion correction," *In: Proc. of the 17th IEEE International Conference on Image Processing (ICP)*, pp. 4237–4240, Sep. 2010.

[10] F. Devernay and O. Faugeras, "Straight lines have to be straight," *Machine Vision and Applications*, vol. 13, no. 1, pp. 14–24, 2001.

[11] L. Alvarez, L. Gomez, and R. Sendra, "An algebraic approach to lens distortion by line rectification," *Journal of Mathematical Imaging and Vision*, vol. 39, no. 1, pp. 36–50, 2008.

[12] L. Alvarez, L. Gomez, and R. Sendra, "Algebraic lens distortion model estimation," *Image Processing On Line*, vol. 1, 2010.

[13] F. Bukhari and M. Dailey, "Automatic radial distortion estimation from a single image," *Journal of Mathematical Imaging and Vision*, vol. 45, no. 1, pp. 31–45, 2012.

[14] R. Grompone, P. Monasse, J. M. Morel, and Z. Tang, "Lens distortion correction with a calibration harp," *In: Proc. of the 18th IEEE International Conference on Image Processing (ICP)*, pp. 617–620, Sep. 2011.

[15] Z. Tang, R. Grompone von Gioi, P. Monasse, and J.-M. Morel, "High-precision camera distortion measurements with a calibration harp," *JOSA A*, vol. 29, no. 10, pp. 2134–2143, 2012.

[16] C. Ricolfe-Viala and A.-J. Sanchez-Salmeron, "Lens distortion models evaluation," *Appl. Opt.*, vol. 49, no. 30, pp. 5914–5928, Oct 2010.

[17] C. Ricolfe-Viala and A.-J. Sánchez-Salmerón, "Robust metric calibration of non-linear camera lens distortion," *Pattern Recognition*, vol. 43, no. 4, pp. 1688–1699, Apr. 2010.

[18] C. Ricolfe-Viala and A.-J. Sánchez-Salmerón, "Using the camera pin-hole model restrictions to calibrate the lens distortion model," *Optics & Laser Technology*, vol. 43, no. 6, pp. 996 – 1005, 2011.

[19] C. Ricolfe-Viala, A.-J. Sanchez-Salmeron, and E. Martinez-Berti, "Accurate calibration with highly distorted images," *Appl. Opt.*, vol. 51, no. 1, pp. 89–101, Jan 2012.

[20] X. Liu and S. Fang, "Correcting large lens radial distortion using epipolar constraint," *Appl. Opt.*, vol. 53, no. 31, pp. 7355–7361, Nov 2014.

[21] D. Gonzalez-Aguilera, J. Gomez-Lahoz, and P. Rodriguez-Gonzalvez, "An automatic approach for radial lens distortion correction from a single image," *IEEE Sensors Journal 11*, vol. 11, no. 4, pp. 956–965, 2011.

[22] C. Ricolfe-Viala, A. J. Sanchez-Salmeron, and A. Valera, "Efficient lens distortion correction for decoupling in calibration of wide angle lens cameras," *IEEE Sensors Journal*, vol. 13, no. 2, pp. 854–863, 2013.

[23] D. Santana-Cedrés, L. Gomez, M. Alemán-Flores, A. Salgado, J. Esclarín, L. Mazorra, and L. Alvarez, "Invertibility and estimation of two-parameter polynomial and division lens distortion models," *SIAM Journal on Imaging Sciences*, vol. 8, no. 3, pp. 1574–1606, 2015.

[24] D. Santana-Cedrés, L. Gomez, M. Alemán-Flores, A. Salgado, J. Esclarín, L. Mazorra, and L. Alvarez, "An iterative optimization algorithm for lens distortion correction using two-parameter models (companion paper)," *IPOL Image Processing On Line*.

[25] O. Faugeras, *Three-dimensional computer vision*. MIT Press, 1993.

[26] M. Alemán-Flores, L. Alvarez, L. Gomez, and D. Santana-Cedrés, "Automatic corner matching in highly distorted images of zhang's calibration pattern," in *CIARP 2014, 19th Iberoamerican Congress on Pattern Recognition, At Puerto Vallarta - Mexico*, no. 8827. Lecture Notes in Computer Science, Springer, 2014, pp. 754–761.

[27] M. Alemán-Flores, L. Alvarez, L. Gomez, P. Henriquez, and L. Mazorra, "Camera calibration in sport event scenarios," *Pattern Recognition*, vol. 47, no. 1, pp. 89 – 95, 2014.

[28] R. I. Hartley and A. Zisserman, *Multiple view geometry in computer vision*. Cambridge University Press, 2004.

Daniel Santana-Cedrés has received a M.Sc. in Computer Science in October 2011, a M.Sc. in Intelligent Systems and Numerical Applications in Engineering in January 2013, and a Ph.D. in Computer Science in April 2016, all of them from the University of Las Palmas de Gran Canaria. Since 2012, he is member of the Imaging Technology Center (CTIM). His main research interest area is lens distortion model estimation.

Luis Gomez received the Ph.D. degree in telecommunication engineering from the University of Las Palmas de Gran Canaria, Las Palmas de Gran Canaria, Spain. Since 1994, he has been an Associate Professor with the Department of Electronic Engineering and Automatic (DIEA), University of Las Palmas de Gran Canaria. His research interests include image processing (computer vision), remote sensing for SAR, and polarimetric SAR (PolSAR). Dr. Gomez is currently Associate Editor of IEEE Geoscience and Remote Sensing Letters and belongs to the Editorial Board of Image Processing on Line (www.ipol.im).

Miguel Alemán-Flores received his M.Sc. and Ph.D. degrees in Computer Science from the University of Las Palmas de Gran Canaria (Spain) in 1995 and 2002, respectively. Since 2008 he is tenured lecturer at the University of Las Palmas of Gran Canaria. His main research areas are image processing, computer vision and medical imaging.

Agustín Salgado received the M.S. and the Ph.D. degrees in computer science from the University of Las Palmas de Gran Canaria (ULPGC) in 2003 and 2010, respectively. He has spent several postdoctoral periods at Image Processing Group, in the Pompeu Fabra University (Barcelona) and at the CMLA laboratory, in the Ecole Normale Superiéure de Cachan. Currently, he is Assistant Professor at the ULPGC and research member of the Centro de Tecnologás de la Imagen (CTIM). His research areas are focused on optical flow, stereoscopic vision and 3D reconstruction.

Julio Esclarín has received a M.Sc.in mathematics in 1979 from Zaragoza University (Spain) and a Ph.D. in computer science in 1996 from the University of Las Palmas of Gran Canaria (ULPGC, Spain). Since 1998 he is tenured lecturer at the ULPGC. His main research interest areas are the applications of mathematical analysis to computer visin and medical imaging.

Luis Mazorra has received a M.Sc.in mathematics in 1980 from La Laguna University (Spain) and a Ph.D. in computer science in 1994 from University of Las Palmas of Gran Canaria (ULPGC, Spain). Since 1996 he is tenured lecturer at the ULPGC. His main research interest areas are the applications of mathematical analysis to computer vision.

Luis Alvarez has received a M.Sc.in applied mathematics in 1985 and a Ph.D. in mathematics in 1988, both from Complutense University (Madrid, Spain). In 1991/1992 he worked as post-doctoral researcher at CEREMADE laboratory in the computer vision research group directed by Prof. Jean-Michel Morel in Paris. Since 2000 he is full professor at the University of Las Palmas of Gran Canaria (ULPGC). His main research interest areas are the applications of mathematical analysis to computer vision.